Supporting Information: Mass Spectrometric Sampling of a Liquid Surface by Nanoliter Droplet Generation from Bursting Bubbles and Focused Acoustic Pulses: Application to Studies of Interfacial Chemistry

Daniel A. Thomas,[†] Lingtao Wang,[‡] Byoungsook Goh,[†,§] Eun Sok Kim,[‡] J. L. Beauchamp[†]*

† Arthur Amos Noyes Laboratory of Chemical Physics, California Institute of Technology, Pasadena, California 91125

‡ Department of Electrical Engineering-Electrophysics, University of Southern California, Los Angeles, California 90089

Table of Contents

Preferential Ionization of Surface-Active Species

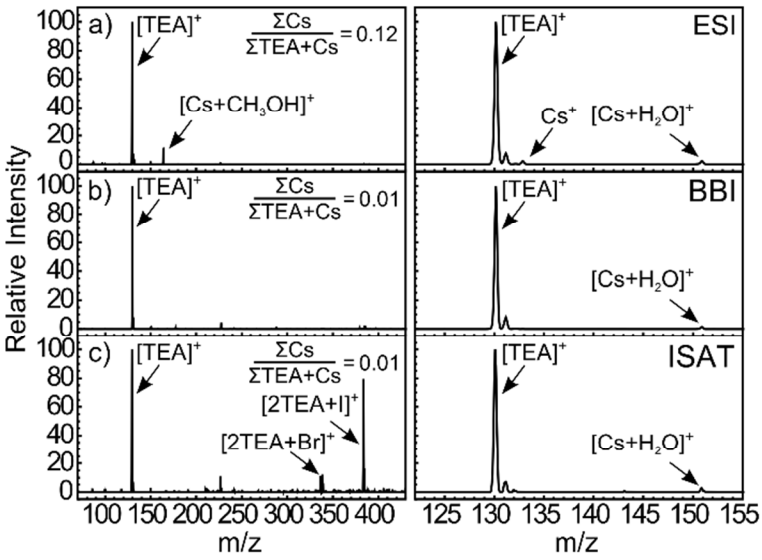

Figure S1. Mass spectra of a solution of tetraethylammonium bromide (TEAB) and cesium iodide at a concentration of 10^{-4} M each utilizing (a) ESI, (b) BBI, and (c) ISAT. The left column shows the full spectrum, while the right column displays only the low-mass region. The response of cesium-associated ions relative to ions of tetraethylammonium is reduced in BBI and ISAT in comparison to ESI (methanol adducts are observed in ESI due to the addition of methanol to this sample to lower surface tension). Significant abundance of halide-bound dimers of tetraethylammnonium is observed in the ISAT spectrum. Given the preferential ionization of large halide anions observed in negative mode, the formation of these dimers is likely to result from an enrichment in the concentration of these species relative to the bulk solution, either in the initial ejected droplet or as a result of the ion desolvation process.

Rayleigh Limit Calculations

The Rayleigh limit for droplet discharge is given by[1-3]

$$Q_R = 8\pi(\epsilon_0 \gamma r^3)^{1/2} \qquad (1)$$

where Q_R is the charge on the droplet, ϵ_0 is the vacuum permittivity, γ is the droplet surface tension, and r is the droplet radius. The surface tension of water at 25° C was taken from Vargaftik *et al.*[4] and utilized for all calculations. For the values presented in Table 1 in the main text, the calculated charge per droplet was divided by the droplet charge at the Rayleigh limit (Q_R) to obtain the percentage of the Rayleigh limit for the droplet.

To estimate the size of droplets produced by BBI, stills were taken from the high speed video (240 frames per second, Canon 510HS) of droplets being ejected. The size of droplets produced by the ISAT device was measured utilizing a microscope connected to a CCD camera as described previously.[5,6] Briefly, a light-emitting diode (LED) was pulsed in synchronization with the RF pulse driving droplet ejection in the ISAT device. A delay time controller introduced a variable time between droplet ejection and LED pulsing to allow for visualization of the generated droplets.

Droplet Residence and Droplet Evaporation Calculations

The transfer time of a droplet through the mass spectrometer inlet capillary is dependent upon the gas flow rate through the inlet, which can be approximated using the Poiseuille equation,[7,8]

$$Q = \frac{\pi r^4}{8\eta L}\Delta P \qquad (2)$$

where ΔP represents the pressure difference across the inlet (759 Torr), r is the radius of the transfer capillary (250 μm), η is the dynamic viscosity of air (2.5×10^{-5} Pa s at 450 K),[9] L is the capillary length (100 mm), and Q is the volumetric flow rate. This equation yields a volumetric gas flow of 4.2×10^{-5} m^3 s^{-1}, or a gas velocity of ~200 m/s and a gas transfer time of ~0.5 ms,

which agrees reasonably well with the gas flow at the MS inlet of ~1 × 10^{-5} m^3 s^{-1} determined with use of a Gilibrator (Sensidyne, St. Petersburg, FL). While this approximation does not take into account the change in gas flow velocity across the transfer tube, the transfer time was also found to be in good agreement with previous studies and serves as an order of magnitude estimate for gas transfer time.[7,10,11]

When the aspirated droplet initially enters the capillary, its velocity along the axis of the capillary is near zero, and the acceleration of the droplet to the carrier gas velocity requires a non-negligible amount of time. This rate of acceleration can be estimated from the drag force F_D exerted on the droplet by the flowing gas, given by[12]

$$F_D = C_D \frac{\pi}{8} \rho_g d^2 \left(v_{gas} - v_{droplet}\right)^2 \qquad (3)$$

where C_D is the coefficient of drag (~0.44 at the high Reynolds numbers encountered in this system),[12] ρ_g is the gas density (~1 kg/m^3),[9] d is the droplet diameter, v_{gas} is the gas velocity, and $v_{droplet}$ is the droplet velocity. Neglecting the effects of turbulent flow, the timescale for droplet transit across the capillary can be estimated by accounting for the acceleration caused by the drag force on the droplet to yield the differential equation

$$m \frac{d^2x}{dt^2} = C_D \frac{\pi}{8} \rho_g d^2 \left(v_{gas} - \frac{dx}{dt}\right)^2 \qquad (4)$$

For a droplet of diameter 100 μm, the calculated transit time across a 100 mm capillary is approximately 15 ms.

The rate of change of a droplet of diameter d due to evaporation is given by[12]

$$\frac{d(d)}{dt} = \frac{4 D_v M}{R \rho_d d} \left(\frac{p_\infty}{T_\infty} - \frac{p_d}{T_d}\right) \qquad (5)$$

where M is the solvent molar mass, D_v is the diffusivity of the solvent vapor in air, ρ_d is the solvent density, and R is the gas constant. The solvent partial pressure at well away from the

droplet surface and at the droplet surface are represented by p_∞ and p_d, respectively, and the corresponding temperatures are denoted by T_∞ and T_d. Integrating this equation yields the droplet evaporation rate as a function of time[12,13]

$$d^2 = d_0^2 + \frac{8D_v M}{R\rho_d}\left(\frac{p_d}{T_d} - \frac{p_\infty}{T_\infty}\right)t \qquad (6)$$

where d_0^2 is the initial droplet diameter. The solvent evaporation process is endothermic, lowering the temperature at the droplet surface, T_d, until equilibrium between evaporative cooling and heat conduction from the surrounding air is achieved. This steady state temperature can be calculated by[12]

$$T_d = T_\infty - \frac{D_v M \Delta H_{vap}}{R k_v}\left(\frac{p_d}{T_d} - \frac{p_\infty}{T_\infty}\right) \qquad (7)$$

where ΔH_{vap} is the solvent enthalpy of vaporization at temperature T_d and k_v is the thermal conductivity of the gas. Since many of the parameters in equation 7 are temperature-dependent, specifically D_v, p_d, ΔH_{vap}, and k_v, the equation must be solved for T_d iteratively until a self-consistent temperature is achieved. The solvent enthalpy of vaporization and equilibrium vapor pressure were taken from Yaws,[14] the diffusion coefficient of water in air was taken from Vargaftik *et al.*,[15] and the thermal conductivity of air was taken from Kadoya *et al.*[16] The value of p_∞ was approximated by the partial pressure of water vapor in air at 50% relative humidity at 298 K,[14] and T_∞ was set to the transfer capillary temperature (450 K). These parameters gave an equilibrium droplet surface temperature, T_d, of 318 K, which was used for the calculation of the droplet diameter as a function of time according to equation 6, with solvent density at this temperature taken from *The CRC Handbook of Chemistry and Physics*.[9]

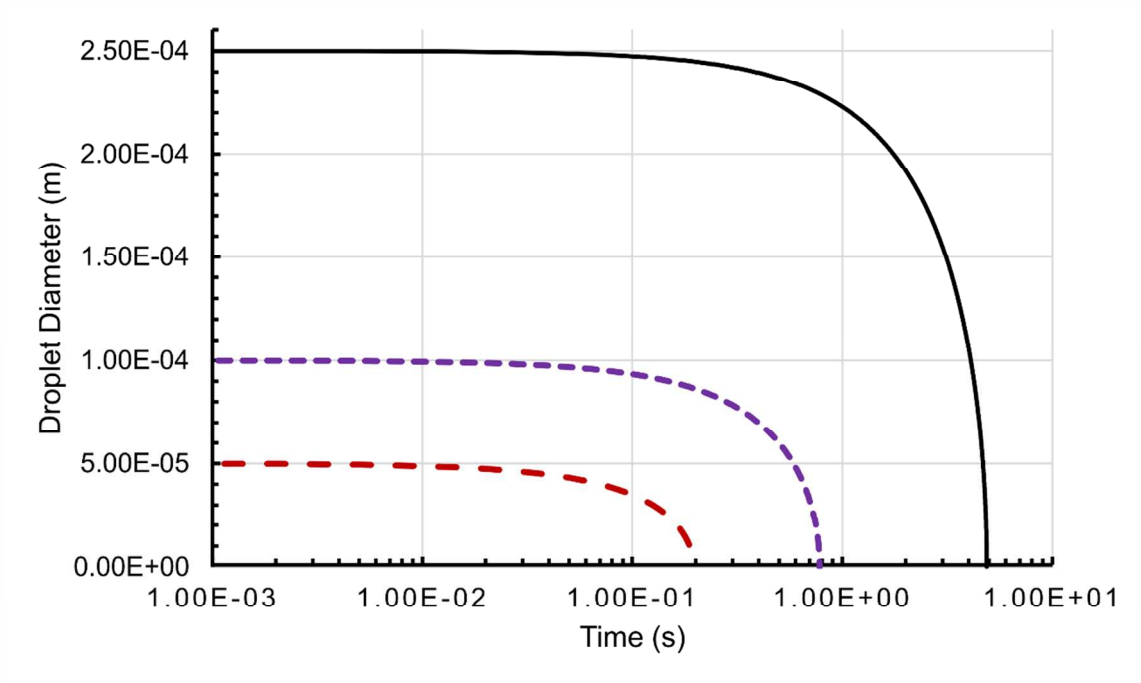

Figure S2. Calculated change in droplet diameter with time for droplets of diameter 50 µm (red, large dash), 100 µm (purple, small dash), and 250 µm (black, solid line) at a gas temperature of 450 K and a water vapor pressure of 1571 Pa (50% relative humidity at 298 K). The time axis is presented on a logarithmic scale. See text for details.

The graph of droplet diameter as a function of time calculated from equations 6 and 7 is shown in Figure S2 for droplets of diameter 50, 100, and 250 µm, which are found to evaporate in 200 ms, 780 ms, and 4.9 s, respectively. For the 100 and 250 µm diameter droplets utilized in this study, the timescale for evaporation is significantly longer than the maximum available transfer time of approximately 15 ms.

References

(1) Rayleigh, L. *Philos. Mag. (1798-1977)* **1882**, *14*, 184-186.
(2) Kebarle, P.; Verkerk, U. H. *Mass Spec. Rev.* **2009**, *28*, 898-917.
(3) Smith, J. N.; Flagan, R. C.; Beauchamp, J. L. *J. Phys. Chem. A* **2002**, *106*, 9957-9967.
(4) Vargaftik, N. B.; Volkov, B. N.; Voljak, L. D. *J. Phys. Chem. Ref. Data* **1983**, *12*, 817-820.
(5) Huang, D.; Kim, E. S. *J. Microelectromech. Syst.* **2001**, *10*, 442-449.
(6) Lingtao, W.; Youngki, C.; Eun Sok, K. In *2011 IEEE 24th International Conference on Micro Electro Mechanical Systems (MEMS)*: Cancun, Mexico, 2011, pp 1115-1118.
(7) Zilch, L. W.; Maze, J. T.; Smith, J. W.; Ewing, G. E.; Jarrold, M. F. *J. Phys. Chem. A* **2008**, *112*, 13352-13363.
(8) Tison, S. A. *Vacuum* **1993**, *44*, 1171-1175.
(9) *CRC Handbook of Chemistry and Physics*, 95th ed.; CRC Press: Boca Raton, 2014.
(10) Gimelshein, N.; Gimelshein, S.; Lilly, T.; Moskovets, E. *J. Am. Soc. Mass Spectrom.* **2014**, *25*, 820-831.
(11) Xu, W.; Charipar, N.; Kirleis, M. A.; Xia, Y.; Ouyang, Z. *Anal. Chem.* **2010**, *82*, 6584-6592.
(12) Hinds, W. C. *Aerosol Technology: Properties, Behavior, and Measurement of Airborne Particles*, 2nd ed.; Wiley: New York, 1999.
(13) Grimm, R. L.; Beauchamp, J. L. *Anal. Chem.* **2002**, *74*, 6291-6297.
(14) Yaws, C. L. *Chemical Properties Handbook: Physical, Thermodynamic, Environmental, Transport, Safety, and Health Related Properties for Organic and Inorganic Chemicals*; McGraw-Hill: New York, 1999.
(15) Vargaftik, N. B.; Vinogradov, Y. K.; Yargin, V. S. *Handbook of Physical Propertieis of Liquids and Gases: Pure Substances and Mixtures*, 3rd ed.; Begell House, Inc.: New York, 1996.
(16) Kadoya, K.; Matsunaga, N.; Nagashima, A. *J. Phys. Chem. Ref. Data* **1985**, *14*, 947-970.